

See discussions, stats, and author profiles for this publication at: <https://www.researchgate.net/publication/281488449>

# Isotropic Undecimated Wavelet Transform Fuzzy Algorithm for Retinal Blood Vessel Segmentation

Article in Journal of Medical Imaging and Health Informatics · November 2015

DOI: 10.1166/jmhi.2015.1561

CITATIONS

19

READS

720

7 authors, including:



**Xingyun Geng**

Nantong University

13 PUBLICATIONS 49 CITATIONS

SEE PROFILE



**Xiaofeng Zhang**

Nantong University

19 PUBLICATIONS 110 CITATIONS

SEE PROFILE



**Lemin Tang**

Nantong University

38 PUBLICATIONS 319 CITATIONS

SEE PROFILE



**Hui-Qun Wu**

Nantong University

96 PUBLICATIONS 946 CITATIONS

SEE PROFILE



# Isotropic Undecimated Wavelet Transform Fuzzy Algorithm for Retinal Blood Vessel Segmentation

Kui Jiang<sup>1</sup>, Zhixing Zhou<sup>1</sup>, Xingyun Geng<sup>1</sup>, Xiaofeng Zhang<sup>1</sup>, Lemin Tang<sup>3</sup>,  
Huiqun Wu<sup>1,2,\*</sup>, and Jiancheng Dong<sup>1,\*</sup>

<sup>1</sup>Department of Medical Informatics, Medical School of Nantong University, 226001, China

<sup>2</sup>Key Laboratory of Medical Imaging Computing and Computer Assisted Intervention (MICCAI) of Shanghai, Fudan University, 200032, China

<sup>3</sup>Department of Medical Image Engineering, Medical School of Nantong University, 226001, China

The segmentation of retinal blood vessels is of significance in retinal image analysis but has some technical difficulties since its easy-to-get noise effect during imaging. In this study, we proposed an isotropic undecimated wavelet transform (IUWT) fuzzy algorithm for retinal blood vessel segmentation. After image preprocessing, we utilized IUWT to denoise the retinal image in its frequency field, and then we performed a robust fuzzy clustering algorithm on texture features based on local gray value entropy to segment retinal blood vessels automatically. Post-processing morphological treatments were performed to refine the segmentation results. Two public datasets were used to test our segmentation method. The sensitivity, specificity and area under receiver operating characteristic curve was 0.8205, 0.9018 and 0.9375 respectively for our proposed method, with time cost about 13.4 s in a personal computer, which is comparable with other algorithms. Therefore, we believed that our proposed algorithm is an available method that could be applied in segmentation for retinal image analysis.

**Keywords:** Retinal Vessel, Texture, Isotropic Undecimated Wavelet Transform, Fuzzy C-Mean Clustering.

## 1. INTRODUCTION

Retinal vessels are micro-blood vessels which could be observed conveniently in a non-invasive way through fundus camera, therefore it's widely used in many clinical departments. The retinal vessel analysis is often conducted by clinicians in their diagnosis and monitoring of chronic systemic diseases such as hypertension, renal failure and diabetes.<sup>1</sup> Unfortunately, a retinal vessel network is so complicated that its analysis by an eye physician is only based on some obvious pathological changes. However, minor changes of retinal vessels could be the early bio-image indicator of chronic diseases like diabetes.<sup>2,3</sup>

Recently, more and more researchers have proposed different approaches for retinal vessel segmentation.<sup>4–8</sup> Moghimirad et al.<sup>9</sup> proposed a multi-scale medialness function to segment retinal vessels, which could get accuracy results, however, it's a bit time-consuming. Similarly, Mendonça et al.<sup>10</sup> detected centerlines of retinal vessels and then made reconstruction of the retinal vessels. Miri and Mahloojifar applied the connected components analysis and length filtering locally instead of the whole image and achieved to more than 94% accuracy for blood vessel detection.<sup>11</sup> Machine learning techniques have also been proposed as solutions. Salem et al.<sup>12</sup> proposed a semi-supervised

clustering method to segment retinal blood vessels. Goatman et al.<sup>13</sup> used a method based on watershed lines and ridge strength measurement, and extracted 15 feature parameters associated with shape, position, orientation, brightness, contrast and line density to obtain candidate segments, then they utilized support vector machine (SVM) classifier to segment retinal vessels. For retinal vessel detection, the performances of a number of vessel segmentation algorithms are always compared on some public datasets.<sup>14</sup> In this study, we proposed a robust fuzzy clustering algorithm on texture features to segment retinal vessels automatically, and tested the algorithm in two public datasets.

## 2. MATERIALS AND METHODS

### 2.1. Fundus Image Dataset

In order to compare the effect of our algorithm with others, we utilized two public international dataset, DRIVE and STARE,<sup>15</sup> which contain normal and abnormal fundus color images respectively together with their manual label results from ophthalmologists which could be recognized as gold standards for comparison.

### 2.2. Isotropic Undecimated Wavelet Transform

In clinics, eye fundus images could be interrupted by different noises during the imaging process, which would affect the

\*Authors to whom correspondence should be addressed.

segmentation accuracy. Therefore, the pre-processing process is essential. In our study, green channel of the color image was firstly abstracted to enhance the contrast of retinal vessels. Then, isotropic undecimated wavelet transform (IUWT) was performed on our tested retinal images.<sup>16,17</sup>

IUWT affords a particularly simple implementation that could be readily appreciated, that is, at each iteration  $j$ , scaling coefficients  $c_j$  are computed by lowpass filtering, and wavelet coefficients  $w_j$  by subtraction. The scaling coefficients were stored as the mean of the original signal, whereas wavelet coefficients encoded information corresponding to different spatial scales present within the signal. Applied to a signal  $c_0 = f$ , subsequent scaling coefficients were calculated by convolution with a filter  $h \uparrow j$ , and wavelet coefficients were the difference between two adjacent iteration of scaling coefficients, which was defined as follows:

$$c_{j+1} = c_j * h \uparrow j \quad (1)$$

$$w_{j+1} = c_j - c_{j-1} \quad (2)$$

where  $h_0 = [1, 4, 6, 4, 1]/16$  was derived from the cubic B-spline, and  $h \uparrow j$  was the upsampled filter obtained by inserting  $2j - 1$  zeros between each pair of adjacent coefficients of  $h_0$ . The final set of scaling coefficients was added after the computation of  $n$  wavelet levels, and reconstruction of the original signal from all wavelet coefficients was defined as follows:

$$f = c_n + \sum_{j=1}^n w_j \quad (3)$$

In this way, the noise as well as some pathological changes in fundus image could be filtered to better segment retinal vessels, with reconstructed image resolution unchanged (Fig. 1). In this study, the 4th level reconstructed image after IUWT showed better contrast in gray-scale image, and was selected for further steps.

### 2.3. Texture Features Extracted Based on Gray Value Entropy

For further blood vessel pixel classification, the gray value of each pixel was obtained, besides, the texture features in retinal

image was also calculated. The image entropy reflects the gray value distribution characteristics, in this study, we considered the gray value entropy neighborhood pixels around the detected pixel as:

$$H = - \sum_{i=0}^{255} p_{ij} \log_2 p_{ij} \quad (4)$$

$$P_{ij} = f(i, j) / N^2 \quad (5)$$

in which  $i$  ( $0 \leq i \leq 255$ ) represents the detected center pixel,  $j$  ( $0 \leq j \leq 255$ ) represents the mean gray value of  $i$ 's neighborhood pixels,  $f(i, j)$  was the frequency of  $(i, j)$ ,  $N$  was defined as the scale of image.

In this way, the texture features of retinal vessels could be extracted for further analysis. In this study, the local entropy of 8 neighborhoods around each image pixel was extracted for further classification.

### 2.4. Fuzzy C-Mean Clustering Method for Retinal Vessel Pixels Classification

Fuzzy C-mean clustering (FCM) analysis is an unsupervised method, which classified samples into different subsets based on their features. Minimum-cost function was used by calculus to obtain the best classification results. Fuzzy collection defines a membership degree function to describe the relationship between member and its subsets. Therefore, the FCM algorithm was used to obtain the best membership degree and clustering centers.<sup>18</sup> In our experiment, cluster number was set as 2 to identify retinal vessel and background,  $m$  as 2, and largest iteration times were set as 100, and classification error was set as 10-5. The above-extracted texture features were classified using FCM for retinal vessel images.

### 2.5. Post-Processing

After pixel clustering, some misclassified pixels need further image processing. In our study, morphological processing erosion and dilation was performed to exclude single pixels, and the structure element was circle with radius as 1.

## 3. EXPERIMENTS AND RESULTS

In this study, we tested our proposed algorithm on Intel Pentium duo core CPU P6000, Windows 7 Home Basic operating system and MATLAB 7.8.0 (R2009a).

To compare our proposed algorithm with other algorithms, we calculated the sensitivity, specificity and draw receiver operator characteristic (ROC) curve of our algorithm. Sensitivity, also named true positive rate (TPR) is the percentage of our segmented retinal vessel pixels in the manually segmented vessel pixels. While specificity, also named true negative rate (TNR), is the percentage of our classified background pixels in the manually classified background pixels. ROC curve is an effective method to evaluate diagnostic tools. It's plotted with sensitivity as a longitudinal axis and 1-specificity as transverse axis. The area under ROC (AUC) could reflect the accuracy of the algorithm too. AUC between 0.5–0.7 means little accuracy, while between 0.7–0.9 as mean accuracy, over 0.9 as higher accuracy.

Compared with manually segmented vessels (usually treated as golden standards), our algorithm could segment the main branches of retinal vessels well (Fig. 2).

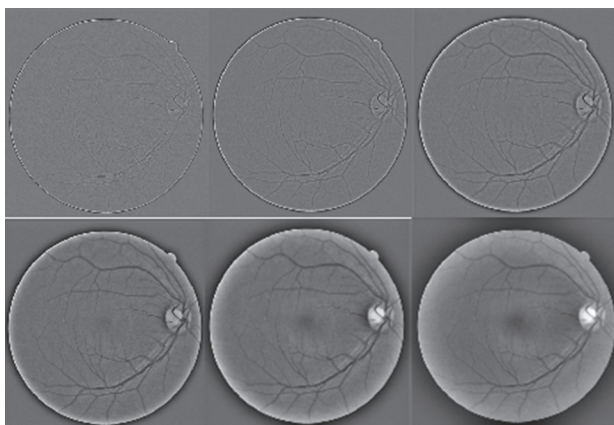


**Fig. 1.** Different layers of retinal images reconstructed after IUWT, the set of wavelet coefficients generated at each iteration is referred to as a wavelet level.

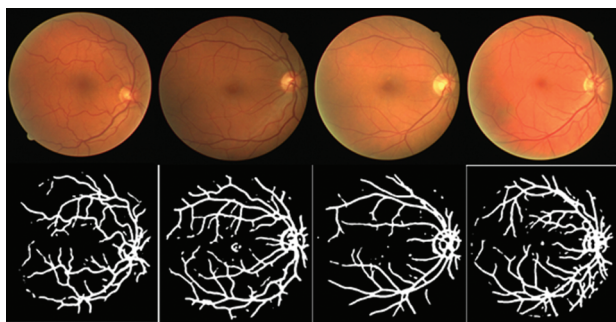


**Fig. 2.** Our segmentation results compared with the manual results from DRIVE dataset (first row: normal fundus images; second row: our segmentation results).

When applied in those pathological fundus images, the main vessels as well as the pathological findings such as bleeding and edema have all been detected, which might affect the final results of accuracy (Fig. 3).

However, the results were still regarded as good after consulting two ophthalmologists.

Compared with other similar studies, our proposed algorithm had highest sensitivity, and AUC was 0.9375, suggesting the applicability of our proposed algorithm (Table I).

The mean time of calculation for a retinal image was 13.4 s, indicating the method is worthwhile for retinal image analysis.

#### 4. DISCUSSION

To those patients with retinal disease, repetitive fundus image tests should be ordered to monitor the disease development. The retinal vessel network and pathological changes are essential for making diagnosis.<sup>19,20</sup> However, the assessment performed by those trained clinicians increased the cost of tests and could be biased by their experiences sometimes. Therefore, an automated protocol is needed to evaluate the retinal networks. A robust segmentation algorithm is of significance for further decision support systems.<sup>21</sup>

In the process of fundus imaging, the causes of uneven illumination, low contrast between vessel and background due to equipment will contribute to the difficulty in vessel segmentation. The retinal vessel itself has the feature of lines, and its cross section intensity presents Gaussian curve distribution, even when

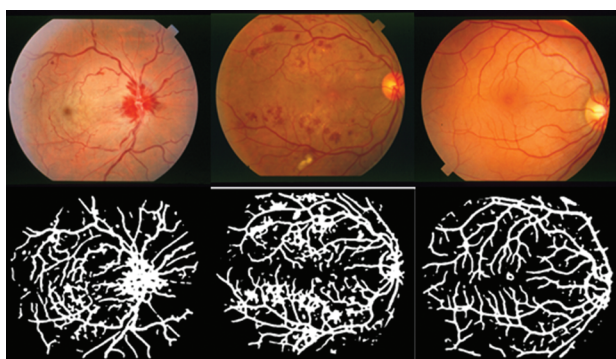


**Fig. 3.** Our segmentation results compared with the manual results from STARE dataset (first row: pathological fundus images; second row: our segmentation results).

**Table I.** The comparison of different algorithms in segmentation.

Algorithm	Sensitivity	1-specificity	AUC
Lupascu et al. <sup>4</sup>	0.6728	0.0126	0.9561
Mendonca and Campilho <sup>5</sup>	0.7315	0.0219	N/A
Staal et al. <sup>6</sup>	0.7194	0.0227	0.9520
Vlachos and Dermatas <sup>7</sup>	0.7468	0.0450	N/A
Zhang et al. <sup>8</sup>	0.7120	0.0276	N/A
Moghimirad et al. <sup>9</sup>	0.7852	0.0065	0.9580
Our method	0.8205	0.0982	0.9375

being affected by the background and pathological changes. The blood vessel branches from the central optic disc to outside, its width becomes narrow and intensity turns to be low, all making the ending vessels hard to be differentiated.<sup>22</sup>

Our proposed segmentation algorithm based on texture features extraction method is a combination of wavelet transforms, texture entropy, and FCM classifier. The algorithm achieves comparable results in terms of sensitivity, specificity, and ROC curve. The average time for image segmentation is about 13 seconds, which is worthwhile for further retinal vessel analysis. However, our algorithm still has some limitations such as easy local minimum results during FCM calculating, and the discontinuous segmented vessels after skeleton processing, which are in need of further optimum processing and refinement.

#### 5. CONCLUSION

The proposed method is a sensitive and time-saving method for retinal vessel segmentation, which could be applied in retinal image analysis.

**Acknowledgments:** This work was supported by the grant of National Natural Science Foundation of China (No. 81271668) and (No. 81371663) and Pre-research project for Natural Science Foundation of Nantong University (No. 14ZY021).

#### References and Notes

1. G. Garhofer, T. Bek, A. G. Boehm, D. Gherghel, J. Grunwald, P. Jeppesen, H. Kergoat, K. Kotliar, I. Lanzl, J. V. Lovasik, E. Nagel, W. Vilser, S. Orgul, and L. Schmetterer, Use of the retinal vessel analyzer in ocular blood flow research. *Acta Ophthalmol.* 88, 717 (2010).
2. C. R. Buchanan and E. Trucco, Contextual detection of diabetic pathology in wide-field retinal angiograms. *Conf. Proc. IEEE Eng. Med. Biol. Soc.* 2008, 5437 (2008).
3. C. Y. Cheung, E. Lamoureux, M. K. Ikram, M. B. Sasongko, J. Ding, Y. Zheng, P. Mitchell, J. J. Wang, and T. Y. Wong, Retinal vascular geometry in Asian persons with diabetes and retinopathy. *J. Diabetes Sci. Technol.* 6, 595 (2012).
4. C. A. Lupascu, D. Tegolo, and E. Trucco, FABC: Retinal vessel segmentation using AdaBoost. *IEEE Trans. Inf. Technol. Biomed.* 14, 1267 (2010).
5. A. M. Mendonca and A. Campilho, Segmentation of retinal blood vessels by combining the detection of center lines and morphological reconstruction. *IEEE Trans. Med. Imag.* 25, 1200 (2006).
6. J. Staal, M. D. Abramoff, M. Niemeijer, M. A. Viergever, and B. van Ginneken, Ridge-based vessel segmentation in color images of the retina. *IEEE Trans. Med. Imaging* 23, 501 (2004).
7. M. Vlachos and E. Dermatas, Multi-scale retinal vessel segmentation using line tracking. *Comput. Med. Imag. Graph.* 34, 213 (2010).
8. B. Zhang, L. Zhang, L. Zhang, and F. Karray, Retinal vessel extraction by matched filter with first-order derivative of Gaussian. *Comput. Biol. Med.* 40, 438 (2010).
9. E. Moghimirad, S. H. Rezaatofghi, and H. Soltanian-Zadeh, Retinal vessel segmentation using a multi-scale medialness function. *Comput. Biol. Med.* 42, 50 (2012).
10. A. M. Mendonça and A. Campilho, Segmentation of retinal blood vessels by combining the detection of centerlines and morphological reconstruction. *IEEE Trans. Med. Imaging* 25, 1200 (2006).

11. M. S. Miri and A. Mahloojifar, Retinal image analysis using curvelet transform and multistructure elements morphology by reconstruction. *IEEE Trans. Biomed. Eng.* 58, 1183 (2011).
12. S. A. Salem, N. M. Salem, and A. K. Nandi, Segmentation of retinal blood vessels using a novel clustering algorithm (RACAL) with a partial supervision strategy. *Med. Biol. Eng. Comput.* 45, 261 (2007).
13. K. A. Goatman, A. D. Fleming, S. Philip, G. J. Williams, J. A. Olson, and P. F. Sharp, Detection of new vessels on the optic disc using retinal photographs. *IEEE Trans. Med. Imaging* 30, 972 (2011).
14. M. Niemeijer, J. Staal, B. van Ginneken, M. Loog, and M. D. Abràmoff, Comparative study of retinal vessel segmentation methods on a new publicly available database. *Proc. SPIE Med. Imag.* 5370, 648 (2004).
15. DRIVE: Digital Retinal Images for Vessel Extraction, Website, <http://www.isi.uu.nl/Research/Databases/DRIVE/Last> Visit: November (2012).
16. P. Bankhead, C. N. Scholfield, J. G. McGeown, and T. M. Curtis, Fast retinal vessel detection and measurement using wavelets and edge location refinement. *PLoS One*. 7, e32435 (2012).
17. J. L. Starck, J. Fadili, and F. Murtagh, The undecimated wavelet decomposition and its reconstruction. *IEEE Trans. Signal Process* 16, 297 (2007).
18. N. Dey, A. B. Roy, M. Pal, and A. Das, FCM based blood vessel segmentation method for retinal images. *Intern. J. Comp. Sci. Net.* 1, 148 (2012).
19. N. Cheung, S. L. Rogers, K. C. Donaghue, A. J. Jenkins, G. Tikellis, and T. Y. Wong, Retinal arteriolar dilation predicts retinopathy in adolescents with type 1 diabetes. *Diabetes Care* 31, 1842 (2008).
20. J. M. Kim, M. Sae Kim, K. Ho Park, and J. Caprioli, The association between retinal vessel diameter and retinal nerve fiber layer thickness in asymmetric normal tension glaucoma patients. *Invest. Ophthalmol. Vis. Sci.* 53, 5609 (2012).
21. G. Dougherty, M. J. Johnson, and M. D. Wiers, Measurement of retinal vascular tortuosity and its application to retinal pathologies. *Med. Biol. Eng. Comput.* 48, 87 (2010).
22. K. A. Vermeer, F. M. Vos, and H. G. Lemij, and A. M. Vossepoel, A model based method for retinal blood vessel detection. *Comput. Biol. Med.* 34, 209 (2004).

Received: 16 February 2015. Revised/Accepted: 30 April 2015.

Delivered by Publishing Technology to: Huiqun Wu  
IP: 127.0.0.1 On: Fri, 01 Apr 2016 06:30:59  
Copyright: American Scientific Publishers